Eddy saturation and frictional control of the Antarctic Circumpolar Current

Marshall, D. P., Ambaum, M. H. P., Maddison, J. R., Munday, D. R. and Novakova, L. (2017) Eddy saturation and frictional control of the Antarctic Circumpolar Current. Geophysical Research Letters, 44 (1). pp. 286-292. ISSN 0094-8276 doi: https://doi.org/10.1002/2016GL071702 Available at https://centaur.reading.ac.uk/68869/

AGU PUBLICATIONS

Geophysical Research Letters

RESEARCH LETTER
10.1002/2016GL071702

Key Points:
- The physics of eddy saturation is explained from first principles
- Enhanced bottom drag increases eddy energy dissipation and hence circumpolar volume transport
- Eddy energy dissipation may have an important impact on ocean heat tcontent and atmospheric CO_2

Supporting Information:
- Supporting Information S1

Correspondence to:
D. P. Marshall,
david.marshall@physics.ox.ac.uk

Citation:
Marshall, D. P., M. H. P. Ambaum, J. R. Maddison, D. R. Munday, and L. Novak (2017), Eddy saturation and frictional control of the Antarctic Circumpolar Current, *Geophys. Res. Lett.*, *44*, 286–292, doi:10.1002/2016GL071702.

Received 23 OCT 2016
Accepted 19 DEC 2016
Accepted article online 21 DEC 2016
Published online 9 JAN 2017

Eddy saturation and frictional control of the Antarctic Circumpolar Current

David P. Marshall[1], Maarten H. P. Ambaum[2], James R. Maddison[3], David R. Munday[4], and Lenka Novak[2]

[1]Department of Physics, University of Oxford, Oxford, UK, [2]Department of Meteorology, University of Reading, Reading, UK, [3]School of Mathematics and Maxwell Institute for Mathematical Sciences, University of Edinburgh, Edinburgh, UK, [4]British Antarctic Survey, Cambridge, UK

Abstract The Antarctic Circumpolar Current is the strongest current in the ocean and has a pivotal impact on ocean stratification, heat content, and carbon content. The circumpolar volume transport is relatively insensitive to surface wind forcing in models that resolve turbulent ocean eddies, a process termed "eddy saturation." Here a simple model is presented that explains the physics of eddy saturation with three ingredients: a momentum budget, a relation between the eddy form stress and eddy energy, and an eddy energy budget. The model explains both the insensitivity of circumpolar volume transport to surface wind stress and the increase of eddy energy with wind stress. The model further predicts that circumpolar transport increases with increased bottom friction, a counterintuitive result that is confirmed in eddy-permitting calculations. These results suggest an unexpected and important impact of eddy energy dissipation, through bottom drag or lee wave generation, on ocean stratification, ocean heat content, and potentially atmospheric CO_2.

1. Introduction

The Antarctic Circumpolar Current (ACC) is driven by wind and buoyancy forcing [e.g., *Rintoul and Naveira Garabato*, 2013] with a modest contribution from remote diapycnal mixing [*Munday et al*., 2011]. However, numerous studies have shown that its equilibrium volume transport is much less sensitive to the surface wind stress in eddy-saturated models with resolved, rather than parameterized, turbulent ocean eddies [*Straub*, 1993; *Hallberg and Gnanadesikan*, 2001; *Tansley and Marshall*, 2001; *Hallberg and Gnanadesikan*, 2006; *Munday et al*., 2013].

Understanding the processes that control eddy saturation is important because the ACC volume transport is closely tied to global ocean stratification [*Gnanadesikan and Hallberg*, 2000; *Karsten et al*., 2003; *Munday et al*., 2011] and thereby to ocean heat and carbon storage [*Ferrari et al*., 2014; *Munday et al*., 2014; *Watson et al*., 2015; *Lauderdale et al*., 2016]. The majority of ocean circulation models used for climate projections do not resolve eddies and show much greater sensitivity of the ACC volume transport and overturning to the surface wind stress [*Farneti and Delworth*, 2010; *Farneti et al*., 2015; *Bishop et al*., 2016; *Gent*, 2016], calling into question the ability of current coupled climate models to reliably predict future ocean heat and carbon uptake [e.g., *Le Quéré et al*., 2007; *Farneti et al*., 2010].

The aims of this study are to explain the physics of eddy saturation and to demonstrate that this leads to anti-frictional control—stronger dissipation results in a stronger ACC—with important implications for ocean heat and carbon content.

2. Simple Model of Eddy Saturation

The model of eddy saturation requires just three ingredients: a zonal momentum budget, a relation between the eddy form stress and the eddy energy, and an eddy energy budget. The model is inspired by a previous model of variability in atmospheric storm tracks [*Ambaum and Novak*, 2014]. In order to keep the model analytically tractable, we impose uniform stratification and constant rotation: the key qualitative results do not appear to be dependent on these assumptions, although the quantitative details will undoubtedly change, in particular with more realistic stratification profiles.

The first ingredient is the zonal momentum budget (Figure 1). Over the Southern Ocean, the input of eastward momentum from the surface wind stress, τ_s, is balanced by loss of momentum to the solid Earth

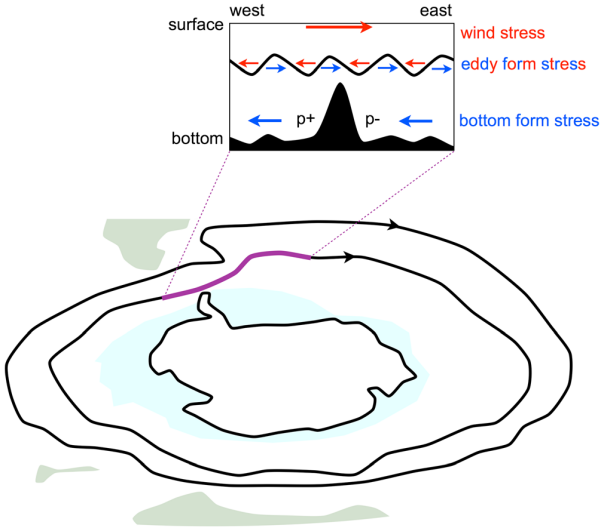

Figure 1. Schematic of the zonal momentum balance of the ACC. Along a time-mean streamline (thick black lines), the eastward surface wind stress (thick red arrow, rectangular insert) is balanced by a bottom form stress (thick blue arrows), associated with a high ($p+$) and low ($p-$) pressure forming upstream and downstream of topographic obstacles such as Drake Passage. Momentum is transferred down from the surface to the seafloor through an eddy form stress, by fluid in upper buoyant layers pushing against the fluid in deeper dense layers (thin red and blue arrows, the undulating black line representing the interface between the buoyant and dense layers), and additionally by the Coriolis forces associated with any residual overturning (not shown).

through a bottom form stress [*Munk and Palmén*, 1951]. The bottom form stress involves high and low pressures forming to either side of the Drake Passage and other topographic barriers, and hence deceleration of the abyssal flow. To connect the surface wind and bottom form stresses, momentum must be transferred down from the surface to the seafloor. This is achieved primarily through an eddy form stress, S [*Johnson and Bryden*, 1989; *Olbers*, 1998]; analogous to the bottom form stress, fluid in more buoyant layers pushes against fluid in less buoyant layers. In addition, momentum is transferred vertically by the Coriolis forces associated with any residual overturning [*Marshall*, 1997; *Marshall and Radko*, 2003], $-\rho\,|f|\,\psi$, where ψ is the streamfunction for the residual overturning, ρ is the density of seawater, and f is the Coriolis parameter (negative in the ACC). In equilibrium, the surface wind stress equals the sum of the eddy form stress and the residual Coriolis force,

$$\tau_s = S - \rho\,|f|\psi. \tag{1}$$

The second and key new ingredient, following *Marshall et al.* [2012], is that the dimensional magnitude of the eddy form stress is set by the eddy energy, E,

$$S = \alpha_1 \frac{|f|}{N} E, \tag{2}$$

where N is the buoyancy frequency and $\alpha_1 \leq 1$ is a nondimensional parameter. Substituting (2) into the momentum balance (1), it follows that the eddy energy is set by the surface wind stress, with an offset due to residual overturning:

$$E = \frac{1}{\alpha_1}\frac{N}{|f|}\tau_s + \frac{\rho N}{\alpha_1}\psi. \tag{3}$$

The third and final ingredient is the eddy energy budget. The dominant source of eddy energy in the Southern Ocean is baroclinic instability of the ACC [e.g., *Rintoul and Naveira Garabato*, 2013]. For an ocean with uniform stratification and shear, the source of eddy energy scales with the mean vertical shear $\partial u/\partial z$ and the eddy energy, i.e.,

$$\text{eddy energy source} = \alpha_2 \frac{|f|}{N}\frac{\partial u}{\partial z}\int_{-H}^{0} E\,dz, \tag{4}$$

where the integral is from the seafloor, $z = -H$, to the sea surface, $z = 0$ (see *Marshall et al.* [2012] for a derivation) and $\alpha_2 \leq 1$. Note that the growth rate of eddy energy is equal to the Eady energy growth rate for linear instability if $\alpha_2 = 0.61$ [*Eady*, 1949].

The physics of eddy energy dissipation remains hotly debated [e.g., *Naveira Garabato et al.*, 2004; *Molemaker et al.*, 2005; *Sen et al.*, 2008; *Zhai et al.*, 2010; *Nikurashin and Ferrari*, 2010; *Melet et al.*, 2015]. Here we sidestep the detailed physics by introducing an eddy energy damping rate, λ, which multiplies the depth-integrated eddy energy, i.e.,

$$\text{eddy energy sink} = \lambda \int_{-H}^{0} E\, dz. \tag{5}$$

Equating the source and sink of eddy energy, (4) and (5), and noting that both depend on the eddy energy which therefore factors out, the eddy energy balance reduces to

$$\alpha_2 \frac{|f|}{N}\frac{\partial u}{\partial z} = \lambda. \tag{6}$$

Assuming that the zonal velocity vanishes at the seafloor, the mean velocity is $\frac{1}{2} H\, \partial u/\partial z$. Integrating across the channel, of width L, the circumpolar volume transport is therefore

$$T = \lambda \frac{N}{|f|}\frac{H^2 L}{2\alpha_2}. \tag{7}$$

Note that, in reality, the bottom velocity may account for up to 25% of the total ACC volume transport [*Peña-Molino et al.*, 2014], and hence, (7) should be interpreted as a prediction for the thermal wind volume transport relative to the seafloor.

Thus, in this simple model, both the vertical shear and the circumpolar volume transport are independent of the surface wind stress and set by the damping rate of eddy energy. In the Southern Ocean, eddy energy is dissipated primarily by bottom drag [*Sen et al.*, 2008] and scattering into lee waves [*Naveira Garabato et al.*, 2004; *Nikurashin and Ferrari*, 2010; *Melet et al.*, 2015], and it is these two processes that we infer may set the ACC volume transport.

In summary, the simple model of the ACC suggests that the momentum budget sets its eddy energy (3) and the eddy energy budget sets its momentum (7). Physically, the equilibrium volume transport is controlled by the ACC requiring sufficiently unstable vertical shear to overcome the stabilizing role of the eddy energy dissipation, a balance that is independent of the wind forcing in this simple model. This behavior is analogous to the interplay between wave activity and baroclinicity in atmospheric storm tracks [*Ambaum and Novak*, 2014].

3. Numerical Calculations

The model makes the counterintuitive prediction that the ACC volume transport increases with increased dissipation. To test this result, a series of eddy-resolving calculations are presented in an idealized channel with an imposed surface wind stress and single topographic barrier.

The numerical model is an idealized eddy-resolving (10 km grid spacing) configuration of the MITgcm [*Marshall et al.*, 1997], previously used to study the impact of the Drake Passage and Tasman Gateway on the ACC [*Munday et al.*, 2015], to which the reader is referred for full model details and parameters. The configuration used in this study is that with a single topographic obstacle in the form of a 1.5 km high topographic ridge; the channel is otherwise 3 km deep, 9600 km long, and 2000 km wide. The ridge is sufficiently high so as to block all f/H contours where H is ocean depth.

A sinusoidal wind stress is imposed at the surface, varying from zero at the southern and northern boundaries to a maximum in the center of the channel. The surface temperature is restored to a linear surface profile, which ranges from 0°C at the southern boundary to 15°C at the northern boundary. Diapycnal mixing is weak, except near the northern boundary where it is enhanced to represent diapycnal mixing in Atlantic and Pacific basins [*Munday et al.*, 2011]. Linear bottom friction with a constant coefficient is applied in the locally deepest level which away from the ridge is the bottom level; over the ridge, the deepest level is higher in the water column and may have reduced thickness due to the use of partial bottom cells and the variable layer thickness, from 10 m at the surface to 250 m in the deepest level. Each of the calculations is run for sufficiently long to reach statistical equilibrium.

The results are shown in Figure 2. These confirm that for all but the smallest bottom drag, the eddy energy increases with wind stress but is independent of bottom drag; in contrast, the volume transport is relatively independent of wind stress and increases with bottom drag. The strengthening of the ACC with larger bottom drag is due to the latter suppressing the growth of turbulent eddies. A similar result was obtained by

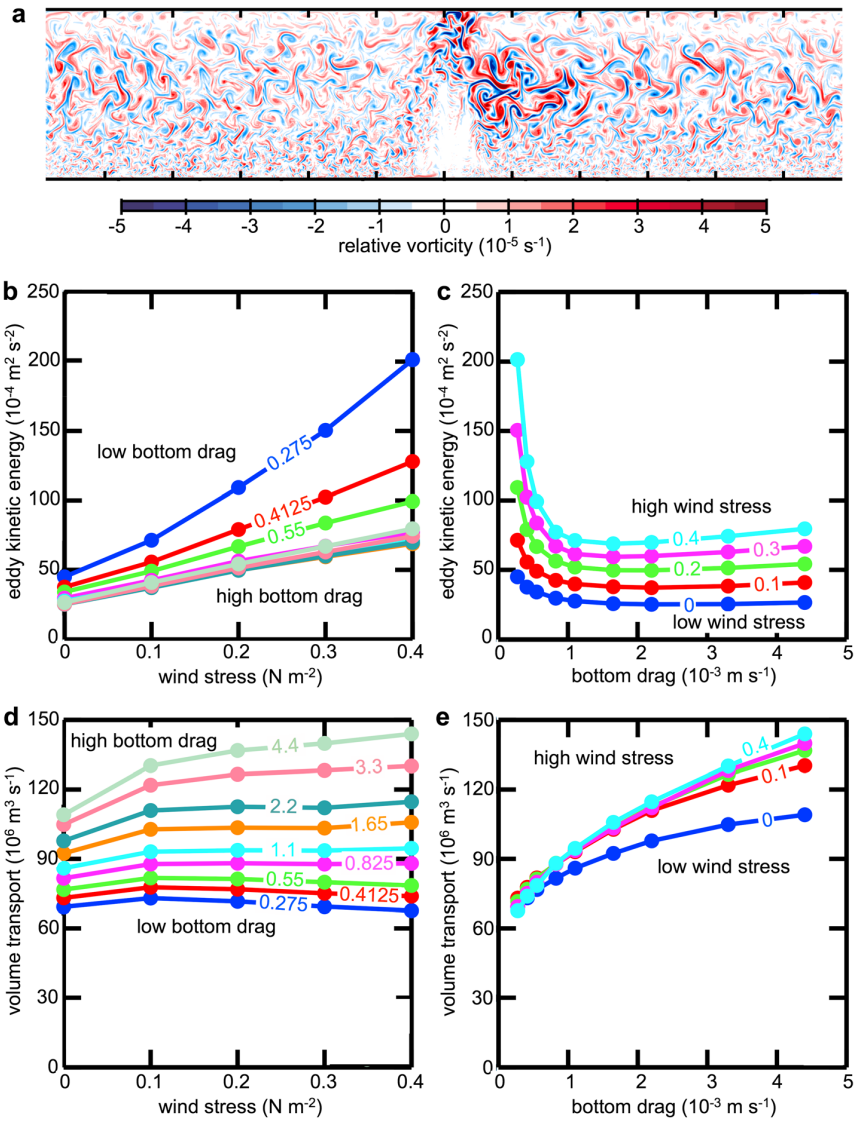

Figure 2. Numerical calculations exploring sensitivity of circumpolar volume transport and eddy energy to surface wind stress and bottom drag. (a) Snapshot of the relative vorticity revealing an energetic field of mesoscale eddies. (b) Eddy kinetic energy as a function of wind stress for different values of bottom drag (10^{-3} m s^{-1}). (c) Eddy kinetic energy as a function of bottom drag for different values of wind stress (N m^{-2}). (d) Volume transport as a function of wind stress for different values of bottom drag. (e) Volume transport as a function of bottom drag for different values of wind stress. (The bottom drag coefficients are equal to the damping rate of momentum within the lowest layer multiplied by 250 m, the latter representing the default lowest layer thickness.)

Nadeau and Ferrari [2015] and was implicit in *Cessi* [2008], although its climatic significance appears to have been overlooked. The broad consistency of these numerical results with the simple theoretical predictions (equations (1) and (2)) is remarkable given the large spatial variations in eddy energy obtained in the numerical solutions (see supporting information).

4. Implications for Ocean Stratification and Heat Content

The strength of the ACC is coupled to the slope of the density surfaces across the Southern Ocean which, in turn, assuming that the sea surface temperature and density are strongly constrained by air-sea surface

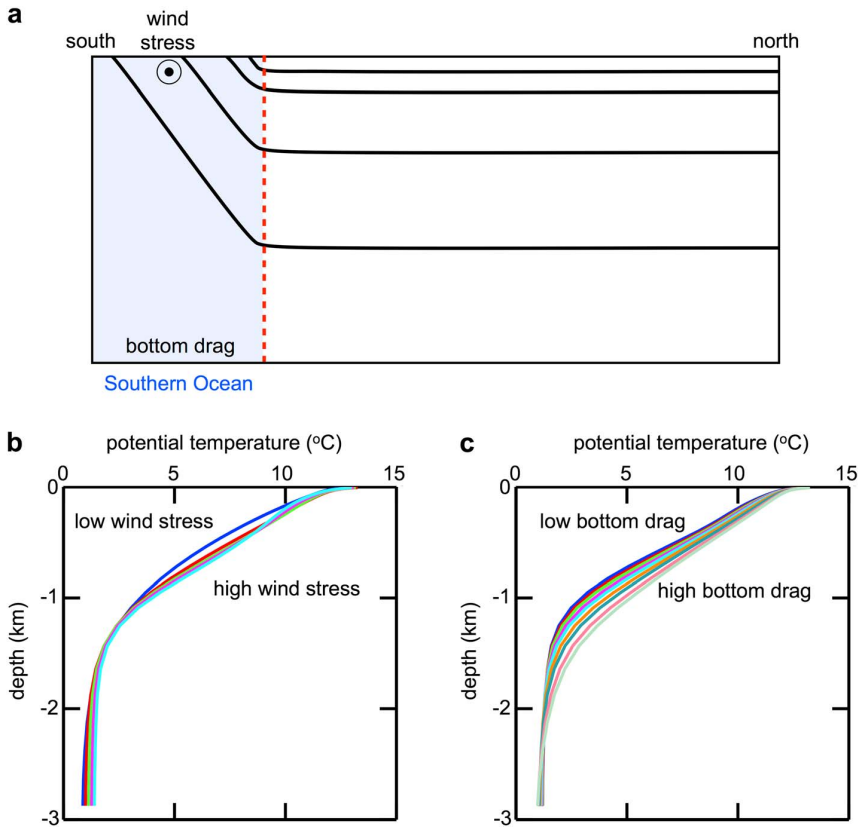

Figure 3. Relation between ocean stratification, surface wind stress, and bottom drag. (a) Schematic illustrating the relation between global stratification and the ACC volume transport, set by the slope of the density surfaces (thick black lines) in the Southern Ocean (blue shading). Increased bottom drag leads to a stronger ACC, steeper density surfaces, and deepened stratification. In contrast, the stratification is relatively insensitive to the wind stress. (b) Variation of potential temperature with depth at the northern edge of the numerical model, corresponding to the red dashed line in Figure 3a, for different values of wind stress. (c) Variation of potential temperature with depth at the northern edge of the numerical model for different values of bottom drag. The line colors in Figures 3b and 3c are the same as in Figure 2.

fluxes, sets the depth of the density surfaces in the basins to the north [*Gnanadesikan*, 1999; *Gnanadesikan and Hallberg*, 2000; *Karsten et al*., 2003; *Nikurashin and Vallis*, 2011; *Marshall and Zanna*, 2014], as sketched in Figure 3a. Thus, a corollary of the results presented in sections 2 and 3 is that eddy energy dissipation in the Southern Ocean, through bottom drag [*Sen et al*., 2008] and scattering into lee waves [*Naveira Garabato et al*., 2004; *Nikurashin and Ferrari*, 2010; *Melet et al*., 2015], may play an important role in setting global ocean stratification and heat content [also see *Cessi et al*., 2006].

This hypothesis can be tested in the eddy-permitting model calculations by examining the sensitivity of the potential temperature profile at the north of the channel to the surface wind stress and bottom drag. We find that this northern potential temperature profile varies weakly with surface wind stress (Figure 3b) but strongly with bottom drag (Figure 3c). Higher bottom drag leads to deeper stratification and increased ocean heat content, consistent with a stronger ACC.

5. Conclusions

A simple theoretical model has been presented that explains the physics of eddy saturation from first principles. The model explains both the insensitivity of circumpolar volume transport to surface wind stress and the increase of eddy energy with wind stress. The model further predicts that circumpolar transport increases with increased bottom friction, a counterintuitive result that has been confirmed qualitatively in eddy-permitting calculations.

Despite the qualitative agreement between the theoretical model and the eddy-permitting calculations, the theoretical model has a number of shortcomings, including the assumption of constant buoyancy frequency, the assumption of a linear eddy energy damping, and the neglect of lateral variations in eddy energy. For example, it is clear that the simple theory breaks down in the limit of low bottom drag where the eddy energy is far greater in the eddy-permitting calculations than the theory predicts. A further limitation is that residual overturning is not independent of the surface wind stress: a detailed physical explanation of eddy compensation, and its relation to eddy saturation, remains outstanding.

Perhaps the most acute limitation of the theoretical model is the assumption that the dissipation of eddy energy through bottom friction (or other processes) can be related in a simple manner to the depth-integrated eddy energy. For example, the results of *Jansen et al*. [2015] demonstrate that the bottom drag and damping rate of depth-integrated eddy energy can become decoupled in baroclinic flow since the eddy energy dissipation rate due to bottom drag depends on the bottom, rather than the depth-integrated, eddy energy.

A novel aspect of the theoretical model is that it bypasses the need for a diffusive eddy closure. Nevertheless, the approach taken here can be used to infer an eddy diffusivity for use in an eddy closure based on *Gent and McWilliams* [1990]. The predicted eddy diffusivity is tested against diagnosed eddy fluxes for a nonlinear baroclinic instability problem in *Bachman et al*. [2017]: good agreement is obtained across 4 orders of magnitude of variation in the eddy diffusivity, suggesting that it may be possible to capture the physics of eddy saturation in models with parameterized eddies (work in progress).

Due to the close relation between the volume transport of the ACC and the stratification in the basins north, a corollary of this study is that eddy energy dissipation in the Southern Ocean plays a major role in setting global ocean stratification and ocean heat content. To the extent that ocean stratification influences the ocean carbon cycle [*Ferrari et al*., 2014; *Munday et al*., 2014; *Watson et al*., 2015; *Lauderdale et al*., 2016], these results may point to a further unexpected impact of bottom drag and lee wave generation on equilibrium atmospheric CO_2.

Acknowledgments
The comments of Fabian Roquet, Gurvan Madec, and an anonymous reviewer are greatly appreciated and led to an improved final manuscript. We acknowledge funding from the UK Natural Environment Research Council (NE/L005166/1 and NE/M014932/1). This work used the ARCHER UK National Supercomputing Service (http://www.archer.ac.uk). The source code for the model used in this study, the MITgcm, is freely available at http://mitgcm.org. The input files necessary to reproduce the experiments are available from the authors upon request. The authors declare no conflicts of interest.

References

Ambaum, M. H. P., and L. Novak (2014), A nonlinear oscillator describing storm track variability, *Q. J. R. Meteorol. Soc.*, *140*, 2680–2684.
Bachman, S. D., D. P. Marshall, J. R. Maddison, and J. Mak (2017), Evaluation of a scalar eddy transport coefficient based on geometric constraints, *Ocean Modell.*, *109*, 44–54.
Bishop, S. P., et al. (2016), Southern Ocean overturning compensation in an eddy-resolving climate simulation, *J. Phys. Oceanogr.*, *46*, 1575–1592.
Cessi, P. (2008), An energy-constrained parameterization of eddy buoyancy flux, *J. Phys. Oceanogr.*, *38*, 1807–1819.
Cessi, P., W. R. Young, and J. A. Polton (2006), Control of large-scale heat transport by small-scale mixing, *J. Phys. Oceanogr.*, *36*, 1877–1894.
Eady, E. T. (1949), Long waves and cyclone waves, *Tellus*, *1*, 33–52.
Farneti, R., and T. L. Delworth (2010), The role of mesoscale eddies in the remote oceanic response to altered southern hemisphere winds, *J. Phys. Oceanogr.*, *40*, 2348–2354.
Farneti, R., T. L. Delworth, A. J. Rosati, S. M. Griffies, and F. Zeng (2010), The role of mesoscale eddies in the rectification of the Southern Ocean response to climate change, *J. Phys. Oceanogr.*, *40*, 1539–1557.
Farneti, R., et al. (2015), An assessment of Antarctic Circumpolar Current and Southern Ocean meridional overturning circulation during 1958–2007 in a suite of interannual CORE-II simulations, *Ocean Modell.*, *93*, 84–120.
Ferrari, R., et al. (2014), Antarctic sea ice control on ocean circulation in present and glacial climates, *Proc. Natl. Acad. Sci. U.S.A.*, *111*, 8753–8758.
Gent, P. R. (2016), Effects of southern hemisphere wind changes on the meridional overturning circulation in ocean models, *Ann. Rev. Mar. Sci.*, *8*, 79–94.
Gent, P. R., and J. C. McWilliams (1990), Isopycnal mixing in ocean circulation models, *J. Phys. Oceanogr.*, *20*, 150–155.
Gnanadesikan, A. (1999), A simple predictive model for the structure of the oceanic pycnocline, *Science*, *283*, 2077–2079.
Gnanadesikan, A., and R. W. Hallberg (2000), On the relationship of the circumpolar current to southern hemisphere winds in coarse-resolution ocean models, *J. Phys. Oceanogr.*, *30*, 2013–2034.
Hallberg, R., and A. Gnanadesikan (2001), An exploration of the role of transient eddies in determining the transport of a zonally reentrant current, *J. Phys. Oceanogr.*, *31*, 3312–3330.
Hallberg, R., and A. Gnanadesikan (2006), The role of eddies in determining the structure and response of the wind-driven southern hemisphere overturning: Results from the Modeling Eddies in the Southern Ocean (MESO) project, *J. Phys. Oceanogr.*, *36*, 2232–2252.
Jansen, M. F., A. J. Adcroft, R. Hallberg, and I. M. Held (2015), Parameterization of eddy fluxes based on a mesoscale energy budget, *Ocean Modell.*, *92*, 28–41.
Johnson, G. C., and H. L. Bryden (1989), On the size of the Antarctic Circumpolar Current, *Deep Sea Res.*, *36*, 39–53.
Karsten, R., H. Jones, and J. Marshall (2003), The role of eddy transfer in setting the stratification and transport of a circumpolar current, *J. Phys. Oceanogr.*, *34*, 2341–2354.
Lauderdale, J. M., R. G. Williams, D. R. Munday, and D. P. Marshall (2016), The impact of Southern Ocean residual upwelling on atmospheric CO_2 on centennial and millennial timescales, *Climate Dyn.*, doi:10.1007/s00382-016-3163-y.
Le Quéré, C., et al. (2007), Saturation of the Southern Ocean CO_2 sink due to recent climate change, *Science*, *316*, 1735–1738.

Marshall, D. (1997), Subduction of water masses in an eddying ocean, *J. Mar. Res.*, *55*, 201–222.
Marshall, D. P., and L. Zanna (2014), A conceptual model of ocean heat uptake under climate change, *J. Clim.*, *27*, 8444–8465.
Marshall, D. P., J. R. Maddison, and P. S. Berloff (2012), A framework for parameterizing eddy potential vorticity fluxes, *J. Phys. Oceanogr.*, *42*, 539–557.
Marshall, J., and T. Radko (2003), Residual-mean solutions for the Antarctic Circumpolar Current and its associated overturning circulation, *J. Phys. Oceanogr.*, *34*, 2341–2354.
Marshall, J., A. Adcroft, C. Hill, L. Perelman, and C. Heisey (1997), A finite volume, incompressible Navier-Stokes model for studies of the ocean on parallel computers, *J. Geophys. Res.*, *102*, 5753–5766, doi:10.1029/96JC02775.
Melet, A. R., R. Hallberg, A. Adcroft, M. Nikurashin, and S. Legg (2015), Energy flux into internal lee waves: sensitivity to future climate changes using linear theory and a climate model, *J. Clim.*, *28*, 2365–2384.
Molemaker, M. J., J. C. McWilliams, and I. Yavneh (2005), Baroclinic instability and loss of balance, *J. Phys. Oceanogr.*, *35*, 1505–1517.
Munday, D. R., L. C. Allison, H. L. Johnson, and D. P. Marshall (2011), Remote forcing of the Antarctic Circumpolar Current by diapycnal mixing, *Geophys. Res. Lett.*, *38*, L08609, doi:10.1029/2011GL046849.
Munday, D. R., H. L. Johnson, and D. P. Marshall (2013), Eddy saturation of equilibrated circumpolar currents, *J. Phys. Oceanogr.*, *43*, 507–532.
Munday, D. R., H. L. Johnson, and D. P. Marshall (2014), Impacts of effects of mesoscale ocean eddies on ocean carbon storage and atmospheric pCO_2, *Global Biogeochem. Cycles*, *28*, 877–896, doi:10.1002/2014GB004836.
Munday, D. R., H. L. Johnson, and D. P. Marshall (2015), The role of ocean gateways in the dynamics and sensitivity to wind stress of the early Antarctic Circumpolar Current, *Paleoceanography*, *30*, 284–302, doi:10.1002/2014PA002675.
Munk, W. H., and E. Palmén (1951), Note on the dynamics of the Antarctic Circumpolar Current, *Tellus*, *3*, 53–55.
Nadeau, L.-P., and R. Ferrari (2015), The role of closed gyres in setting the zonal transport of the Antarctic Circumpolar Current, *J. Phys. Oceanogr.*, *45*, 1491–1509.
Naveira Garabato, A. C., K. L. Polzin, B. A. King, K. J. Heywood, and M. Visbeck (2004), Widespead intense turbulent mixing in the Southern Ocean, *Science*, *303*, 210–213.
Nikurashin, M., and R. Ferrari (2010), Radiation and dissipation of internal waves generated by geostrophic motions impinging on small-scale topography: Application to the Southern Ocean, *J. Phys. Oceanogr.*, *40*, 2025–2042.
Nikurashin, M., and G. Vallis (2011), A theory of deep stratification and overturning circulation in the ocean, *J. Phys. Oceanogr.*, *41*, 485–502.
Olbers, D. (1998), Comments on "On the obscurantist physics of 'form drag' in theorizing about the circumpolar current", *J. Phys. Oceanogr.*, *28*, 1647–1654.
Peña-Molino, B., S. R. Rintoul, and M. R. Mazloff (2014), Barotropic and baroclinic constributions to along-stream and across-stream transport in the Antarctic Circumpolar Current, *J. Geophys. Res. Oceans*, *119*, 8011–8028, doi:10.1002/2014JC010020.
Rintoul, S. R., and A. C. Naveira Garabato (2013), Dynamics of the Southern Ocean circulation, in *Ocean Circulation and Climate, A 21st Century Perspective*, edited by G. Siedler et al., pp. 471–492, Elsevier, Amsterdam.
Sen, A., R. B. Scott, and B. K. Arbic (2008), Global energy dissipation rate of deep-ocean low-frequency flows by quadratic bottom boundary layer drag: Computations from current-meter data, *Geophys. Res. Lett.*, *35*, L09606, doi:10.1029/2008GL033407.
Straub, D. N. (1993), On the transport and angular momentum balance of channel models of the Antarctic Circumpolar Current, *J. Phys. Oceanogr.*, *23*, 776–782.
Tansley, C. E., and D. P. Marshall (2001), On the dynamics of wind-driven circumpolar currents, *J. Phys. Oceanogr.*, *31*, 3258–3273.
Watson, A., G. K. Vallis, and M. Nikurashin (2015), Southern Ocean buoyancy forcing of ocean ventilation and glacial atmospheric CO_2, *Nat. Geosci.*, *8*, 861–864.
Zhai, X., H. L. Johnson, and D. P. Marshall (2010), Significant sink of ocean-eddy energy near western boundaries, *Nat. Geosci.*, *3*, 608–612.

Geophysical Research Letters

Supporting Information for

Eddy Saturation and Frictional Control of the Antarctic Circumpolar Current

David P. Marshall[1], Maarten H. P. Ambaum[2], James R. Maddison[3], David R. Munday[4], Lenka Novak[2]

[1]Department of Physics, University of Oxford, Oxford, United Kingdom.

[2]Department of Meteorology, University of Reading, Reading, United Kingdom.

[3]School of Mathematics and Maxwell Institute for Mathematical Sciences, University of Edinburgh, Edinburgh, United Kingdom.

[4]British Antarctic Survey, Cambridge, CB3 0ET, United Kingdom.

Contents of this file

Introduction

This supporting information consists of two figures showing variations of the depth-integrated streamfuntion and surface eddy kinetic energy across the numerical calculations reported in sections 3 and 4 of the manuscript.

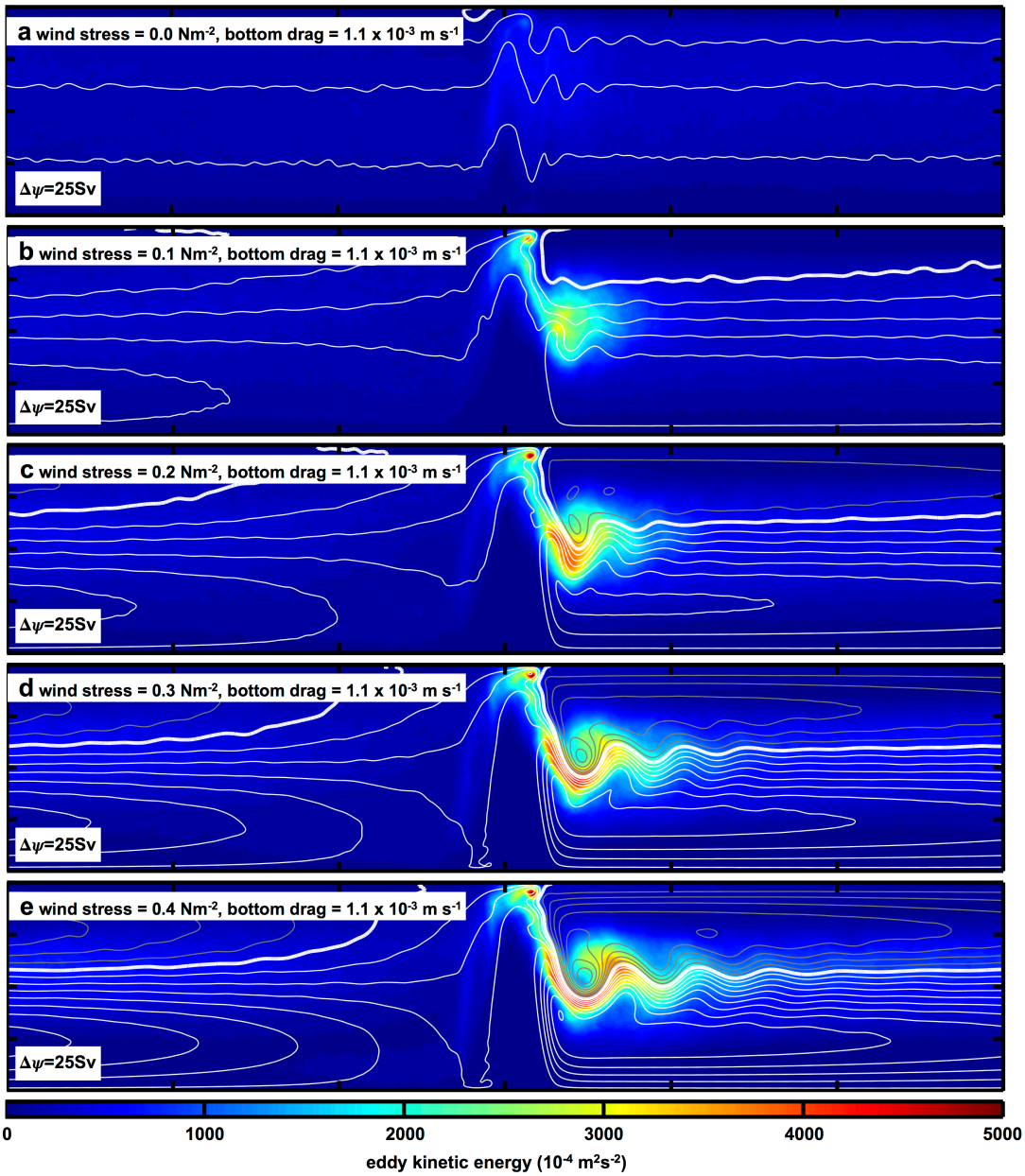

Fig. S1. Variation of the 20-year time averaged depth-integrated streamfunction (lines) and surface eddy kinetic energy density (colors) with wind stress. The thick white contour is at 0 Sv (1 Sv = 10^6 m^3 s^{-1}) with grey/thin white contours representing negative/positive values of streamfunction spaced 25 Sv apart. The peak surface wind stress is labelled on each panel.

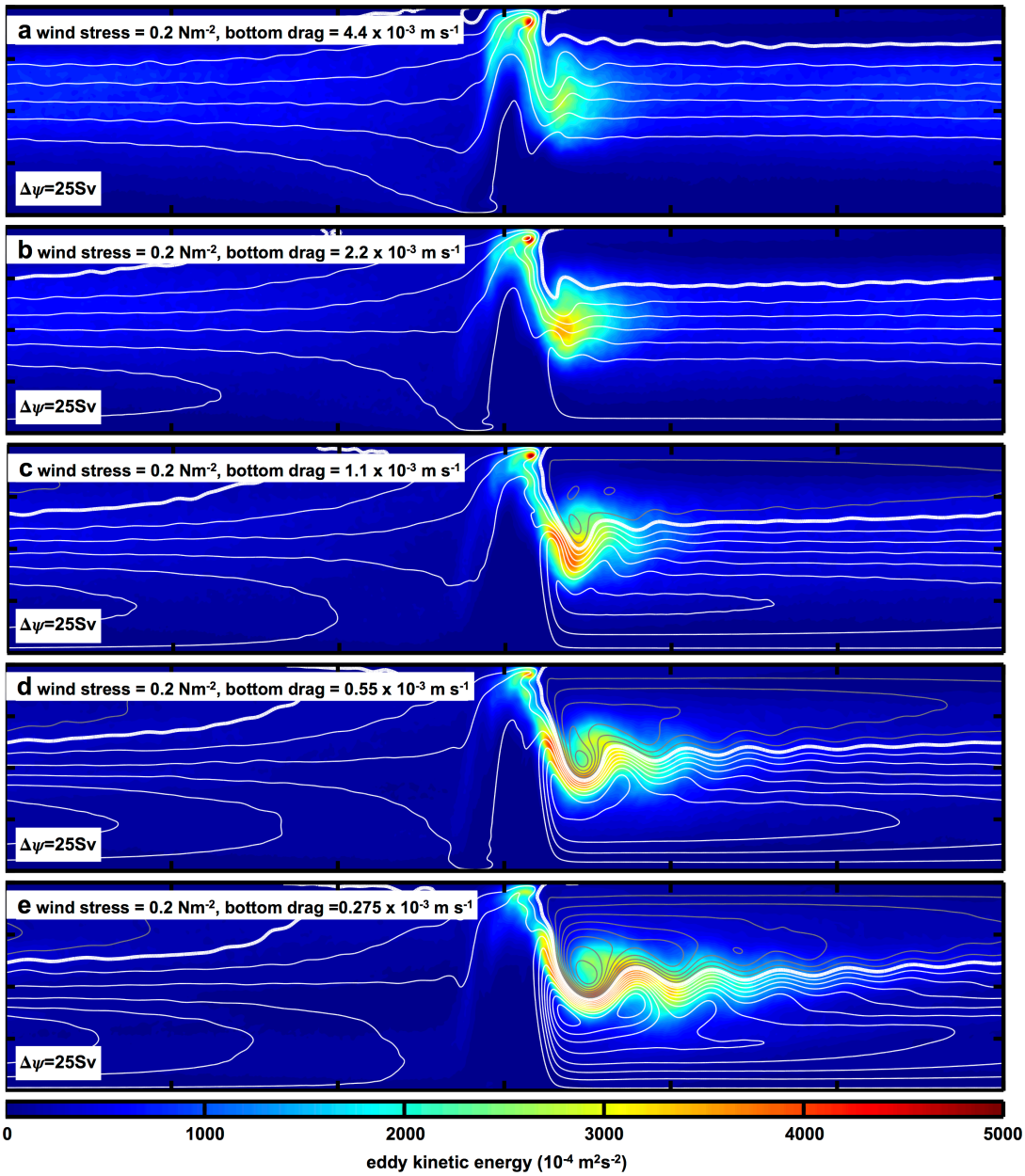

Fig. S2. Variation of the 20-year time averaged depth-integrated streamfunction (lines) and surface eddy kinetic energy density (colors) with bottom friction coefficient. The thick white contour is at 0 Sv with grey/thin white contours being negative/positive values of streamfunction spaced 25 Sv apart. The bottom friction coefficient is labelled on each panel.